Evaluation of a Direct-Coupled TDR for Determination of Soil Water Content and Bulk Electrical Conductivity

Robert C. Schwartz[1], Steven R. Evett[1], Scott K. Anderson[2] and David J.Anderson[2]

[1]PO Drawer 10, USDA-ARS, Bushland, TX,

[2]Acclima, Inc., Meridian, ID

ABSTRACT

Signal degradation in coaxial cables and interconnects is a long-standing problem in the practical deployment of time domain reflectometry (TDR) for soil water monitoring. Acclima, Inc. has recently commercialized a TDR sensor (TDR-315)[1] with all electronics required for waveform acquisition embedded in the probe head. We calibrated ten TDR-315 sensors and conventional TDR for apparent permittivity (K_a) and bulk electrical conductivity (σ_a) measurements. Also, soil water content calibrations were completed for a Pullman clay loam soil. Lastly, the sensitivity of K_a to σ_a was examined using a saturated solute displacement experiment with both probe technologies installed in a column packed with Pullman clay loam. A range of σ_a (0.65 to 2.8 dS m^{-1}) was established by equilibrating the column with 0.25 dS m^{-1} $CaCl_2$ and introducing a step pulse of 7.3 dS m^{-1} $CaCl_2$. Permittivity calibrations of the TDR-315 could be accomplished with conventional TDR methods and with similar sampling errors. Conventional calibrations of σ_a using long time amplitudes yielded a linear response for $\sigma_a \leq 3$ dS m^{-1} above which the response was nonlinear. The fitted water content calibrations of the Pullman clay loam for the TDR-315 were nearly indistinguishable from conventional TDR calibrations with similar root mean square errors (0.017 to 0.020 m^3 m^{-3}). Response of the two

[1]The use of trade, firm, or corporation names in this article is for the information and convenience of the reader. Such use does not constitute an official endorsement or approval by the United States Department of Agriculture or the Agricultural Research Service of any product or service to the exclusion of others that may be suitable.

measurement technologies in a lossy soil during changing solution conductivities demonstrated that, in contrast to conventional TDR, travel time measured using acquired TDR-315 waveforms was insensitive to σ_a up to 2.8 dS m^{-1}.

INTRODUCTION

In-situ, nondestructive monitoring of soil water is critical for the evaluation of water, energy and solute fluxes in the field. Innovations in electromagnetic methods that make use of the unique electrical properties of water have revolutionized the measurement, study and management of water within the soil profile. Characterization of material properties using time domain reflectometry (TDR), initially for determining the dielectric properties of liquids (Fellner-Feldegg, 1969), has become widely accepted for monitoring soil water since its introduction (Hoekstra and Delaney, 1974) and the seminal work by Topp et al. (1980). The fundamental success of the TDR method for estimating soil water content arises from an apparent permittivity (K_a) response that is less sensitive to bulk electrical conductivity (σ_a) compared with lower frequency (< 100 MHz) electromagnetic techniques (Robinson et al., 2003). In addition, minimal soil disturbance using open-ended rods, the ability to measure σ_a (Dalton et al., 1986), and the approximately linear relationship between the water content and the square root of K_a (Ferré and Topp, 2002) or the measured travel time (Topp and Reynolds, 1998; Evett et al., 2005) are further advantages of the method.

Despite the above successes and refinements of the TDR technique, use under field conditions is cumbersome because of unavoidable signal attenuation and high frequency filtering in coaxial cables, multiplexers, and interconnects (Logsdon, 2000; Casanova et al., 2013). Even with the use of high quality coaxial cables, the bandwidth can narrow to less than 0.5 GHz at the cable termination from an incident pulse bandwidth of 1.75 GHz (Schwartz et al., 2009a). Further signal attenuation, dispersion, and high frequency filtering by dielectric loss mechanisms, especially in saturated, fine-textured soils, will further reduce the effective bandwidth thereby increasing the K_a sensitivity to σ_a and temperature and reducing accuracy of water content estimations (Schwartz et al, 2009a, b). Auxiliary measurements of σ_a and temperature can be combined with travel time measurements in soil specific water content calibrations to account for signal attenuation (e.g. Schwartz et al., 2009b). However, such modifications in the calibration procedure are difficult in practice to apply under field conditions and are not entirely satisfactory under elevated σ_a levels (Schwartz et al., 2013).

A TDR sensor (TDR-315) has recently been commercialized by Acclima, Inc. that circumvents the problem of maintaining a high frequency signal over long cable distances. All the electronics required for pulse generation and waveform acquisition are embedded in a miniaturized circuit within the probe head, and processed data is transmitted digitally via SDI-12 protocol with cable lengths of at least 60 m possible (SDI-12 Support Group, 2013). The sensor shares some measurement concepts with the earlier time domain transmission (TDT) Acclima sensor (Anderson and Anderson, 2004; Blonquist et al., 2005; Schwartz et al., 2013) but with a greater bandwidth and new electronics to process signals in the reflection mode. Ideally, the TDR-315 would provide the same advantages of conventional TDR without the problems of signal degradation prior to entering the soil test material. However, evaluation of the waveforms and firmware estimated K_a and σ_a over a range of conditions and media are required to ascertain potential limitations of the sensor compared with conventional TDR. Our objectives were to (i) carry out K_a and σ_a calibrations for the TDR-315 using conventional TDR methods, (ii) complete a water content calibration for a fine-textured soil, and (iii) utilize a saturated column displacement experiment to examine the dependency of measured K_a on σ_a while avoiding the confounding effects of soil water content and pore structure changes. In all of these evaluations, TDR-315 responses were compared with conventional TDR.

MATERIALS AND METHODS

Sensor description

Ten TDR-315 sensors were calibrated and evaluated to ascertain their responses to a range of media as compared with two conventional TDR probes. The TDR-315 sensors consisted of a planar three-conductor transmission line 150 mm in length with the incident pulse transmitted in the center rod and two exterior ground rods (Fig. 1). The sensors had rod diameters of 3.2 mm and a rod separation distance of 19 mm that conforms to the recommended ratio of wire separation to wire diameter less than 10 proposed by Knight (1992). All TDR-315 sensors had the same printed circuit assembly consisting of a step function generator, precision time base generator, 5 ps resolution waveform digitizer, thermistor, and communications circuits potted within the sensor head. The TDR circuit for pulse generation and waveform acquisition was directly coupled to the electrodes. The function generator launches a ~3.5 GHz step pulse with a 10 - 90% rise time of 100 ps (20 – 80% rise time of 64 ps). A digitized waveform is constructed by launching a series of step pulses triggered by a timing generator and, for each step pulse, sampling the amplitude of the reflection at successive time increments. A voltage comparator is used to evaluate (digitize) the amplitude of the analog signal compared with reference amplitude at a given time offset. Using a specialized interface, waveforms can be acquired spanning 0 to 20 ns at sampling intervals of 5 ps or greater.

Although full waveforms can be acquired from the TDR-315 using a specialized interface, the design intent is to return to the user only processed data elements. A microprocessor executes firmware stored in on-board memory to acquire the pertinent waveform features, measure temperature, calculate the apparent permittivity (K_a) and bulk electrical conductivity (σ_a), and transmit this information to compliant data loggers using the Serial Digital Interface (SDI) protocol at 1200 baud (SDI-12). Measurement of propagation time is achieved efficiently by first generating a waveform using coarse time increments and identifying a window containing the reflection at the end of the transmission line. This portion of waveform is sampled at finer time resolution for precise determination of the time, t_2, at which the pulse arrives at the end of the probe. The time of pulse arrival within the medium, t_1, is evaluated at a calibrated offset from the launch of the incident wave to determine propagation time, $t_2 - t_1$. Probes are individually calibrated to report accurate K_a and σ_a, and volumetric water content is calculated using a standard mixing model.

Firmware associated with acquisition of the long time amplitude and the σ_a calibration was still under development for the initial eight sensors evaluated in this study (serial numbers (SN) 1 to 6, 684 and 713). In four sensors (SN 684, 713, 729, and 731), the long time amplitude was acquired approximately 3 μs after the incident wave launch and based on microprocessor cycles whereas in the initial six sensors (SN 1to 6) this measurement was unavailable. In the final two sensors (SN 729 and 731) the σ_a was calculated based on the long time amplitude and the Giese and Tiemann (1975) thin section approach. All waveforms were acquired in quadruplicates.

Conventional TDR

Two conventional TDR probes, each with a 8.5-m low-loss coaxial cable (LMR-240, Times Microwave Systems, Wallingford, CT), were evaluated for comparison with the TDR-315 sensors. The probes had rod diameters of 3.2 mm, an outer rod separation distance of 60 mm, and a length of approximately 150 mm. Waveforms were acquired using a cable tester (model 1502C, Tektronix, Beaverton, OR) with an open-ended 1.75 GHz bandwidth and a 10 – 90% rise time of 200 ps. Waveforms were collected in quadruplicate with waveform averaging set to 4 samples in the 1502C. A coaxial cable length of 8.5 m was used in this study because it more properly represented the attenuated signal used to acquire travel times for estimation of soil water contents in the field than would an arbitrarily short cable. The bandwidth associated with the 10–90% rise time of the TDR pulse that arrives at the end of the 8.5-m cable into the probe was estimated to be 820 MHz (Schwartz et al., 2013).

Apparent permittivity calibration

The TDR-315 sensors were calibrated for apparent permittivity (K_a) using waveforms acquired at 20 ps intervals in air and deionized water. Conventional TDR was also calibrated in the same manner using 251-point waveforms in air and water (13.5 and 53.4 ps intervals, respectively). Amplitudes, V, acquired from the TDR-315 were converted to reflection coefficients, ρ as

$$\rho = \frac{2 \cdot V - V_0}{V_0} \tag{1}$$

where V_0 is the measured amplitude at long times (20 ns) in air (open circuit). Limitations associated with the timing circuit prevented the routine acquisition of amplitudes at times greater than 20.4 ns. Short circuit measurements with the TDR-315 by design yield an amplitude of zero at long times. Travel time for both conventional and digital TDR was evaluated using adaptive waveform interpretation with Gaussian filtering (AWIGF) as described by Schwartz et al. (2014). Three AWGIF algorithm parameters were adjusted to accommodate the differences between the TDR-315 and conventional TDR systems. After scaling amplitudes using Eq. (1), AWIGF was implemented for TDR-315 waveforms using a characteristic noise level $\alpha = 0.25$ ns rather than the 0.142 ns (Schwartz et al., 2014) to account for differences between the TDR-315 step pulse generator and the step pulse generator used in metallic cable testers with conventional TDR. In addition, the standard deviation of the Gaussian kernel for the evaluation of t_1 was set to two-thirds of the value used in conventional TDR. This was necessary because the t_1 evaluation for TDR-315 is based on an offset from launch of the incident step pulse rather than, in conventional TDR, the impedance change generated as the signal leaves the cable, with the former having a more abrupt transition. Lastly, the measured maximum amplitude gradient in air associated with the rising limb of the reflection at the termination of the transmission line was set to 1.2 ns^{-1}. All other parameters were set equivalent to the default values used for interpretation of conventional waveforms using the 1502C cable tester (Schwartz et al., 2014).

A calibration in air and water was used to determine an offset t_c and the electrical length L_e of both conventional TDR and TDR-315 probes (Heimovaara, 1993; Schwartz et al., 2014). In conventional TDR probes, t_c is the time between t_1 and the intersection of the tangent lines to the rising limb of the first reflection and the preceding baseline (t_{x1}). Similarly, for TDR-315 sensors, t_c is the time between t_1 and the launch time of the incident wave also evaluated at the intersection of the tangent lines of the step pulse and the preceding baseline (Fig. 2). Calibrations in water were completed at 20 ± 2°C with the temperature dependent apparent permittivity calculated using the empirical expressions of Stogryn (1971; 1995) assuming an effective frequency of 1 GHz.

Bulk electrical conductivity calibration

Conventional TDR and TDR-315 probes were calibrated for bulk electrical conductivity sensing in $CaCl_2$ solutions with electrical conductivities ranging from 100 μS m^{-1} (deionized water) to 7.3 dS m^{-1}. Electrical conductivity of solutions was measured using a bench top meter (WTW Inolab, White Plains, NY) with conductivity reported at ambient temperatures (20°C ± 2°C). Bulk electrical conductivity (σ_a) using the conventional TDR probes was determined using the method of Lin et al. (2008) using open (air) and short circuit measurements to evaluate the scaled reflection coefficient ρ_{scale} at 3 μs that accounts for the instrumental error and cable resistance (Castiglione and Shouse, 2003). After rescaling, the Giese and Tiemann (1975) method

$$\sigma_a = \frac{K_p}{Z_s}\left(\frac{1-\rho_{scale}}{1+\rho_{scale}}\right) \tag{2}$$

was applied to find the slope of the relationship K_p/Z_s using zero-intercept linear regression where K_p is the probe constant (m^{-1}) and Z_s is the source impedance (Ω). Electrical conductivity calibrations for the TDR-315 sensors were completed using the reflection coefficient (Eq. 1) evaluated at 20 ns (all sensors) and at 3 μs (SN 684,713,729, and 731). Noting that

$$\frac{1-\rho}{1+\rho} = \frac{V_0}{V} - 1 \tag{3}$$

when the short circuit amplitude is zero, the Giese and Tiemann Eq. (2) was also used to evaluate the slope K_p/Z_s for TDR-315 calibrations. Firmware-calculated σ_a was being developed concurrently with testing of TDR-315 sensors and was not implemented in SN 1 to 6, 684, and

713. However, firmware in sensors with SN 729 and 731 reported σ_a based on a factory calibration and these values were compared to measured conductivity values of $CaCl_2$ solutions.

Soil water content calibration

Water content calibrations of the Ap horizon (0 – 0.15 m) of the Pullman clay loam (fine, mixed, superactive, thermic Torrertic Paleustoll) were carried out for six TDR-315 sensors (SN 1 to 6) and two conventional TDR probes. The Pullman Ap horizon has a clay content of approximately 390 g kg^{-1} dominated by smectite and mica (Soil Survey Staff, 2008; Schwartz et al., 2009). Packed columns (0.101 m inside diameter by 0.20 m long Schedule 40 rigid polyvinyl chloride) were prepared using soil sieved through a 12.7-mm by 12.7-mm mesh screen. A range of volumetric water contents was achieved by combining air-dry soil with different ratios of deionized water, thoroughly mixing to achieve uniformity, and packing the mixture into the columns to ~160 mm in 20-mm increments. After packing, the probe and sensor rods were installed vertically into the prepared soil columns. Waveforms were acquired at room temperature (20°C), at 6°C (in a refrigerator), and at 40°C (in a water-jacketed incubator) after permitting the packed columns to equilibrate for one day at each temperature regime. The refractive mixing model (Birchak et al., 1974), which assumes a linear relationship between the square root of K_a and water content, was fitted to measured apparent permittivity using measured volumetric water contents. All temperature regimes were included in the calibrations so that the errors associated with the fitted model would be more representative of non-isothermal field conditions. Slopes of the permittivity response to temperature for the Pullman clay loam calibration were evaluated for each water content level using the general linear model analysis of covariance (SAS, 2009) assuming equal slopes among column replicates.

Solute displacement

The dependence of measured apparent permittivity (K_a) on σ_a in a lossy soil was examined for both the TDR-315 and conventional TDR using a near saturated solute displacement experiment. Air-dry Pullman soil was packed in a 0.2 m diam. by 0.20 m long Schedule 40 polyvinyl chloride column in increments of 20 mm to a depth of 0.19 m. A single TDR-315 sensor was installed at a soil depth of 130 mm through a slot machined into the wall of the column with approximately 20 mm of the 60 mm long sensor head containing the circuitry embedded within the soil. Once the sensor was installed, the slot containing the sensor head was sealed with room temperature vulcanizing silicon gasket maker to prevent water from seeping out of the column. Subsequently, soil was carefully packed above the sensor. A single TDR probe with a rod length of 150 mm was installed at a soil depth of 50 mm with the 30 mm long probe head embedded entirely within the soil and the coaxial cable inserted through a hole in the column wall that was sealed to prevent seepage. The remaining soil was packed above the TDR probe to a depth of 190 cm, leaving 10 mm for ponding of water above the soil surface.

The column was slowly saturated with 1.0 mM $CaC1_2$ (σ_s = 0.25 dS m^{-1} at 25°C) through a bottom inlet. Once the column was saturated, downward, vertical flow was established by maintaining a 5-mm head of influent solution above the soil surface using a Mariotte bottle. After equilibration of the flow concentration at the bottom inlet, the influent solution was switched to ~35 mM $CaC1_2$ (σ_s = 7.3 dS m^{-1} at 25°C) and the displacement experiment was continued until effluent attained 7.2 dS m^{-1} after which the influent was again switched back to 1.0 mM $CaCl_2$. The displacement experiment was completed at a near constant temperature (20 ±1°C) for a duration of 12 days after saturation. Further details of the methodology are provided by Schwartz et al. (2013).

RESULTS AND DISCUSSION

Waveforms acquired with the TDR-315 in air and deionized water (Fig. 2) exhibited features similar to conventional TDR (Schwartz et al., 2014) except for the inclusion of the rising edge of the step pulse launched approximately 0.20 ns prior to the pulse arrival within the medium. Waveform distortions immediately after the incident step pulse that oscillated around the steady state unloaded amplitude (overshoot and ringback) were evident in the trace in air (Fig. 2). These features were present in the relevant portions of the waveform required to evaluate travel time in low permittivity media. The waveform interpretation algorithm AWIGF was modified to ensure that the identified time of the amplitude derivative maximum was associated with the time at which the pulse arrives at the end of the transmission line (t_2) rather than overshoot features. This simply involved providing the algorithm with the physical probe length to set the beginning time of the t_2 search window as 0.6 (2 L)/c where c is the speed of light and L is physical probe length. With this modification, the algorithm had no difficulties in identifying t_2 in low permittivity media. The sample standard deviation for the bulk permittivity in water averaged 0.063 and 0.068 relative permittivity units for the TDR-315 and conventional TDR, respectively. The mean of the sample standard deviation in air for the TDR-315 (0.003) was less than that obtained for conventional TDR (0.009) likely because of greater resolution afforded by the faster rise time of the TDR-315 step pulse generator. Electrical length L_e and offset t_c for permittivity calibrations of the TDR-315 and conventional TDR were remarkably similar (Table 1). Variations in calibrated L_e among TDR-315 probes resulted from small variations in the physical rod length and the timing circuit. Probes with serial numbers 684, 713, 729 and 731 exhibit slightly larger offsets (t_c) and earlier pulse launches because of the inclusion of additional rod length within the epoxy head. These manufacturing variations are accommodated in the commercial sensors by the factory calibration process.

The electrical conductivity (EC) calibrations for conventional TDR probes were linear (Fig. 3) with r^2 values exceeding 0.9998 and non-significant y-intercepts ($P > 0.180$). Likewise, the TDR-315 EC calibrations using the 20 ns long time amplitudes were linear with r^2 values exceeding 0.9988, suggesting that the Giese and Tiemann (1975) thin-section approach for estimation of electrical conductivity was appropriate for these sensors. However, the TDR-315 response deviated from linear at electrical conductivities less than 0.2 dS m^{-1} (Fig. 3), yielding significant linear regression y-intercepts ($P < 0.05$). This nonlinearity was likely due to the settling of amplitudes at these low attenuation levels occurring at times greater than 20 ns. Slopes of the EC responses were similar among conventional TDR probes and TDR-315 sensors (Table 1), although the theoretical probe constant K_p of the conventional TDR probes (4.31 m^{-1}) was 1.2 times greater than that of the TDR-315 (3.59 m^{-1}) because of the greater rod spacing of the former. Long time reflection coefficients evaluated from the 3 μs amplitudes reported by the firmware of the newer probes (serial numbers 684,713,729 and 731) were linear at low conductivities, had y-intercepts not significantly different from zero, and slightly greater r^2 values. However, EC calibrations using these amplitudes at 3 μs departed from a linear response at electrical conductivities greater than 3 dS m^{-1} (Fig. 3). Firmware in two of the latest probes evaluated (SN 729 and 731) reported σ_a based on a factory calibration that accounted for this nonlinearity in the response at $\sigma_a > 3$ dS m^{-1}. Electrical conductivity reported by the nonlinear factory calibration had a relative error of ≤ 6.5% in the 0.01 to 7.3 dS m^{-1} range, which was similar to the error observed for the conventional TDR probes evaluated in this study (≤ 5.0%). Of note, however, is that TDR-315 firmware estimates of σ_a are independently predicted values (calibration coefficients and errors were evaluated using different EC data) and, accordingly, would be expected to have greater error compared with error associated with the conventional TDR fit where the same EC data was used for calibration and the determination of error.

The fitted water content calibration for the Pullman clay loam derived from AWIGF K_a estimates using the TDR-315 corresponded closely to the conventional TDR calibration also using AWIGF to evaluate travel time (Fig. 4). The TDR-315 firmware-calculated K_a averaged 95% of the TDR-315 AWIGF-calculated K_a and the two estimates were closely correlated (r^2 = 0.997). Accordingly, the water content calibration obtained from the firmware estimate of K_a was remarkably similar to the AWIGF derived calibrations (Fig. 4). Slopes and intercepts of the three water content calibrations were similar, with RMSE values that ranged from 0.017 to 0.020 m^3 m^{-3}. At the three lowest water contents evaluated for soil water calibrations (0.04, 0.17, and 0.24 m^3 m^{-3}; Fig 4), both conventional TDR and the TDR-315 K_a response to temperature were positive exhibiting slopes ranging from 0.005 to 0.028 °C^{-1}. Except in one case (conventional TDR at θ = 0.17 m^3 m^{-3}), these temperature responses were significant ($P < 0.05$) and indicative of a mechanistic process, possibly related to the change in bound water with temperature (Or and Wraith, 1999). At near saturated water content (θ = 0.47 m^3 m^{-3}), the slope of the K_a – temperature response was positive for conventional TDR (0.054 °C^{-1}) similar to that reported by Schwartz (2009) and likely due to sensitivity to σ_a that varies with temperature (Evett et al., 2005). In contrast, the K_a – temperature response was negative for the TDR-315 (-0.074 °C^{-1}). We interpret this behavior for the TDR-315 to indicate that near saturation, the thermodielectric response was dominated by bulk water resulting in a decrease in K_a with temperature (Or and Wraith, 1999). The factory water content calibration reported by the firmware tended to underestimate soil water content and had a root mean square error of 0.0324 m^3 m^{-3} that was greater than that of the soil specific calibrations (Fig. 4).

A characteristic feature of all displacement experiments in previous evaluations (Schwartz et al., 2013) and in this study was an increase in conventional TDR measured K_a as the high concentration $CaCl_2$ solute front migrated past the probe rods followed by a decline in K_a after the injection of the final 0.25 dS m^{-1} solution (Fig. 5). The measured response arises because of the contribution of low frequency conductive losses to K_a imparted by a lower effective measurement frequency compared with the incident signal (Hook et al., 2004; Schwartz et al., 2013). Apparent permittivity estimated with AWIGF using conventional TDR increased from 32 to 40 after introduction of the 7.3 dS m^{-1} $CaCl_2$ step pulse (Fig. 5). In contrast, K_a estimated using the TDR-315 and also evaluated using AWIGF was insensitive to σ_a (Fig. 5). Both of the above AWIGF-derived estimates of K_a use the default method whereby t_2 is conditionally evaluated using the maximum of the second derivative (Schwartz et al., 2014). Of note, the AWIGF-calculated K_a for the TDR-315 using the conventional method to estimate t_2 (denoted as t_{x2} which is the intersection of the tangents to the baseline and rising limb) resulted in a slight dependence on σ_a (Fig. 5). Likewise the TDR-315 firmware estimates of K_a were slightly sensitive to σ_a and were subject to reduced precision at $\sigma_a > 2$ dS m^{-1} (Fig. 5). Sensitivity of firmware-calculated K_a to σ_a likely results from evaluation of t_2 using t_{x2}. At greater conductivities, we recommend that waveforms be sampled by the firmware using finer time resolutions to improve K_a estimates. The cause of the insensitivity of the TDR-315 measured K_a to σ_a was evident from the waveforms at a high σ_a (2.8 dS m^{-1}). The slope of the reflection at the termination of the rods was four times greater for the TDR-315 waveform compared with that for conventional TDR (Fig. 6) indicating that a greater proportion of the high frequency signal component was preserved by the TDR-315.

CONCLUSIONS

Waveforms acquired using the TDR-315 sensor over a wide range of media properties were similar to those from conventional TDR and interpretable using the same algorithm with minor adjustments in parameters to account for differences in the step pulse. Calibration of K_a could be accomplished with the conventional TDR method using air and water as two known permittivities. The conventional Giese and Tiemann (1975) approach for σ_a calibration gave a linear response to $\sigma_a < 3$ dS m^{-1} for long-time amplitudes obtained at 3 μs. At greater conductivities, the response became nonlinear. Firmware successfully accounted for the nonlinearity and reported electrical conductivities to within 6.5% of a benchtop meter. The fitted water content calibrations for the Pullman clay loam using the firmware-reported K_a and the AWIGF-calculated travel time were both nearly indistinguishable from conventional TDR calibrations. The response of K_a to σ_a in a saturated Pullman clay loam exhibited by the two sensor technologies differed markedly. Waveforms acquired by the TDR-315 probe retained a greater proportion of high frequency components as compared to conventional TDR as was inferred by a greater slope of the reflection at the rod termination. This resulted in AWIGF-derived permittivity measurements from the TDR-315 that were insensitive to σ_a up to 2.8 dS/m and a corresponding pore water conductivity of 7.3 dS/m. In contrast, measured K_a using conventional TDR increased by 25% over the same range in conductivities. Firmware-calculated K_a for the TDR-315 was satisfactory compared with estimates evaluated using AWIGF, although waveforms should be sampled by the firmware at higher time resolutions when $\sigma_a > 2$ dS m^{-1}. Based on these observations, the TDR-315 would be more suitable for measurement of soil water contents in saline or salt affected soils than is conventional TDR. Considering that measured K_a is insensitive to σ_a for the range evaluated in this study, exhibited temperature responses of K_a

for the TDR-315 Pullman water content calibrations are therefore a result of bound water effects and, unlike conventional TDR in lossy, fine-textured soils, not a combination of both σ_a and bound water. For high accuracy water content measurements, we recommend soil specific calibrations using the firmware reported K_a.

ACKNOWLEDGEMENTS

The authors gratefully acknowledge the financial support of USDA SBIR Phase II Contract 2012-02152, NSF SBIR Phase I Contract 1346113, and the International Atomic Energy Agency CRP D1.20.13 Contract 18210/R0. The authors also sincerely acknowledge the assistance of Bridgett DeWitt and Logan Hopper in the completion of laboratory tests. This research was supported by the Ogallala Aquifer Program, a consortium between USDA-Agricultural Research Service, Kansas State University, Texas A&M AgriLife Research, Texas A&M AgriLife Extension Service, Texas Tech University, and West Texas A&M University.

REFERENCES

Anderson, S.K., and H.S. Anderson. 2004. Method and apparatus for determining moisture content and conductivity. U.S. Patent 6831468 B2. Date issued: 14 December.

Birchak, J.R., C.G. Gardner, J.E. Hipp, and J.M. Victor. 1974. High dielectric constant microwave probe for sensing soil moisture. Proc. IEEE 62:93–98.

Blonquist, J.M., Jr., S.B. Jones, and D.A. Robinson. 2005. A time domain transmission sensor with TDR performance characteristics. J. Hydrol. 314:235–245. doi:10.1016/j.jhydrol.2005.04.005

Casanova, J.J., R.C. Schwartz, S.R. Evett, and S. K. Anderson. 2013. Directly coupled vs. conventional time domain reflectometry in soils. Applied Engr. Agric. 29(5): 771-777.

Castiglione, P. and P.J. Shouse. 2003. The effect of ohmic cable losses on time domain reflectometry measurements of electrical conductivity. Soil Sci. Soc. Am. J. 67:414-424.

Dalton, F.N., and M.Th. van Genuchten. 1986. The time-domain reflectometry method for measuring soil water content and salinity. Geoderma 38:237–250.

Evett, S.R., J.A. Tolk, and T.A. Howell. 2005. TDR laboratory calibration in travel time, bulk electrical conductivity, and effective frequency. Vadose Zone J. 4:1020–1029.. doi:10.2136/vzj2005.0046

Ferré, T.P.A. and G.C. Topp. 2002. Time Domain Reflectometry, pp. 434-446. In J.H. Dane, J.H. and G.C. Topp (Eds.), Methods of Soil Analysis. Part 4. Physical Methods. Madison, WI.

Giese, K., and R. Tiemann. 1975. Determination of the complex permittivity from thin-sample time domain reflectometry improved analysis of the step waveform. Adv. Mol. Relax. Processes 7:45-59.

Heimovaara, T.J. 1993. Design of triple-wire time domain reflectometry probes in practice and theory. Soil Sci. Soc. Am. J. 57:1410–1417.doi:10.2136/sssaj1993.03615995005700060003x

Hoekstra, P. and A. Delaney. 1974. Dielectric properties of soils at UHF and microwave frequencies. J. Geophys. Research 79:1699-1708.

Hook, W.R., T.P.A. Ferré, and N.J. Livingston. 2004. The effects of salinity on the accuracy and uncertainty of water content measurements. Soil Sci. Soc. Am. J. 68:47–56.

Knight, J.H. 1992. Sensitivity of time domain reflectometry measurements to lateral variations in soil water content. Water Resour. Res 28:2345-2352.

Lin, C.-P, C.C. Chung, J.A. Huisman, and S.-H. Tang. 2008. Clarification and calibration of reflection coefficient for electrical conductivity measurement by time domain reflectometry. Soil Sci. Soc. Am. J 72:1033-1040.

Logsdon, S.D. 2000. Effect of cable length on time domain reflectometry calibration for high surface area soils. Soil Sci. Soc. Am. J. 64:54-61.

Or, D. and J.M. Wraith. 1999. Temperature effects on soil bulk dielectric permittivity measured by time domain reflectometry: A physical model. Water Resour. Res. 35:371-383.

Robinson, D.A., S.B. Jones, J.M. Wraith, D. Or, and S.P. Friedman. 2003. A review of advances in dielectric and electrical conductivity measurement in soils using time domain reflectometry. Vadose Zone J. 2:444–475.

SAS Institute. 2009. SAS/STAT online documentation. Version 9.2. SAS Inst., Cary. NC.

Schwartz, R.C., J.J. Casanova, J.M. Bell, and S.R. Evett, S.R. 2014. A reevaluation of TDR propagation time determination in soils. Vadose Zone J. doi:10.2136/vzj2013.07.0135

Schwartz, R.C., J.J. Casanova, M.G. Pelletier, S.R. Evett, and R.L. Baumhardt. 2013. Soil permittivity response to bulk electrical conductivity for selected soil water sensors. Vadose Zone J. doi:10.2136/vzj2012.0133.

Schwartz, R.C., Evett, S.R. and Bell, J.M. Complex permittivity model for time domain reflectometry soil water content sensing. II. Calibration. 2009a. Soil Sci. Soc. Am. J. 73(3): 898-909. 2009.

Schwartz, R.C., Evett, S.R., Pelletier, M.G., and Bell, JM. 2009b. Complex permittivity model for time domain reflectometry soil water content sensing. I. Theory. Soil Sci. Soc. Am. J. 73(3):886-897. 2009.

SDI-12 Support Group. 2013. SDI-12 A Serial-Digital Interface Standard for Microprocessor-Based Sensors. Version 1.3. River Heights, Utah. http://www.sdi-12.org/current%20specification/SDI-12_version1_3%20January%2026,%202013.pdf

Stogryn, A.P. 1971. Equations for calculating the dielectric constant of saline water. IEEE Trans. Microw. Theory Tech. 19:733–736.

Stogryn, A.P. 1995. The microwave permittivity of sea and fresh water. GenCorp Aerojet, Azusa, CA.

Topp, G.C., J.L. Davis, and A.P. Annan.1980. Electromagnetic determination of soil-water content: Measurement in coaxial transmission lines. Water Resour. Res. 16:574-582.

Topp, G.C. and W.D. Reynolds. 1998. Time domain reflectometry: a seminal technique for measuring mass and energy in soil. Soil Till. Res 47:125-132.

FIGURE CAPTIONS

Fig. 1. Illustration of a TDR-315 sensor showing electrode length and spacing, sensor head containing the circuitry, and the 3-wire communications cable.

Fig. 2. Waveforms in air and deionized water acquired using a TDR-315 probe showing the time of the step signal launch (t_{x1}), time at which the signal enters the media (t_1) and the time of the reflection at the end of the rod in air, t_2(air), and water t_2(water) determined using AWIGF (Schwartz et al., 2014). The offset, t_c, is fitted based on the calibration in air and water.

Fig. 3. Electrical conductivity (EC) calibrations for the long time reflection coefficient, ρ, in $CaCl_2$ solutions for the TDR and TDR-315. Inset shows calibration response at low EC levels.

Fig. 4. Refractive mixing model soil water content calibrations of the Pullman clay loam (0.0 to 0.15 m) for conventional TDR and TDR-315 using AWIGF-estimated travel times and the apparent permittivity (K_a) calibration (Fig. 2) and the TDR-315 using firmware estimated K_a. Calibrations include permittivity measurements at all three temperature regimes. Also shown is the Acclima factory soil water content calibration.

Fig. 5. Response of electrical conductivity and apparent permittivity during column displacement for conventional TDR and TDR-315 sensors in a Pullman clay loam. Apparent permittivities for the TDR-315 are plotted using two AWIGF methodologies to estimate the time at which the pulse arrives at the end of the transmission line (t_2): the default method that uses the maximum of the second derivative and the conventional method that uses the intersection of the tangents to

the baseline and rising limb (t_{x2}). In addition, firmware-calculated apparent permittivities are also plotted. A lag in the TDR-315 response compared with conventional TDR is due to differing heights within the soil column.

Fig. 6. Waveforms of conventional TDR and the TDR-315 at a bulk electrical conductivity (σ_a) of 2.8 dS m^{-1} and the AWIGF-evaluated time at which the pulse arrives at the end of the transmission line (t_2). The waveforms have been horizontally adjusted in time so that the time at which the step pulse enters the media (t_1) is identical.

Table 1. Apparent permittivity and bulk electrical conductivity calibration parameters for the TDR-315 and conventional TDR. Electrical length (L_e) and offset (t_c) are derived from the air-water calibration. The probe constant divided by the source impedance (K_p/Z_s) is derived from the slope of the long time amplitude calibrations at 20 ns and 3 µs in $CaCl_2$ electrolytic solutions (100 µS m^{-1} to 7.3 dS m^{-1}). The calibration slope for TDR-315 sensors at 3 µs was obtained from the linear range at less than or equal to 3 dS m^{-1} $CaCl_2$.

Serial Number	Physical Length	L_e	t_c	K_p/Z_s 20 ns	K_p/Z_s 3 µs
	m	m	ns	dS m^{-1}	dS m^{-1}
----- Acclima TDR-315 -----					
1	0.150	0.1494	0.189	0.840	
2	0.150	0.1496	0.207	0.917	
3	0.150	0.1489	0.203	0.978	
4	0.150	0.1493	0.206	0.918	
5	0.150	0.1493	0.224	0.923	
6	0.150	0.1498	0.168	0.815	
684	0.145	0.1523	0.243	0.873	0.963
713	0.145	0.1521	0.229	0.850	0.987
729	0.145	0.1535	0.262	0.858	0.974
731	0.145	0.1537	0.236	0.877	0.970
----- Conventional TDR (Tektronix 1502C) -----					
	0.150	0.1550	0.194		0.937
	0.151	0.1570	0.192		0.914

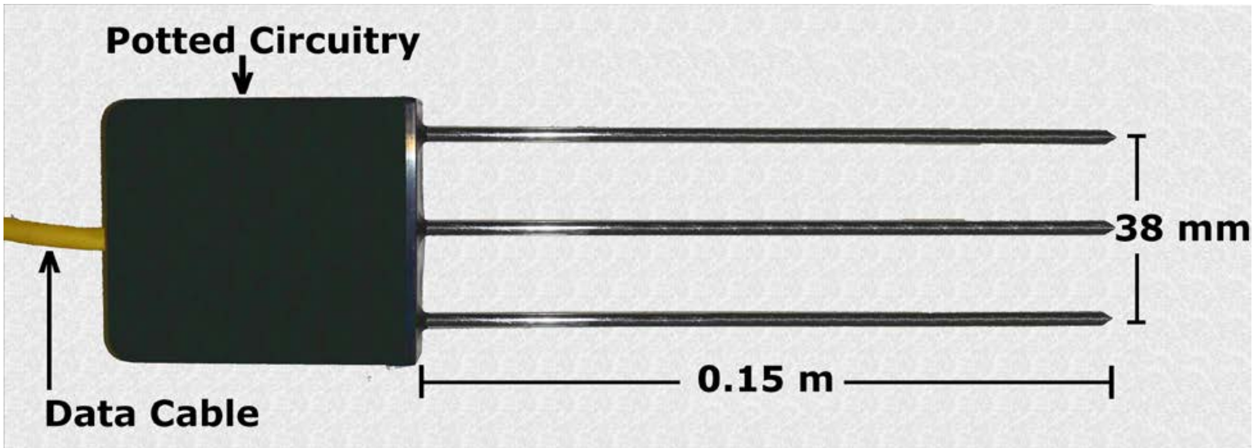

Fig. 1. Illustration of a TDR-315 sensor showing electrode length and spacing, sensor head containing the circuitry, and the 3-wire communications cable.

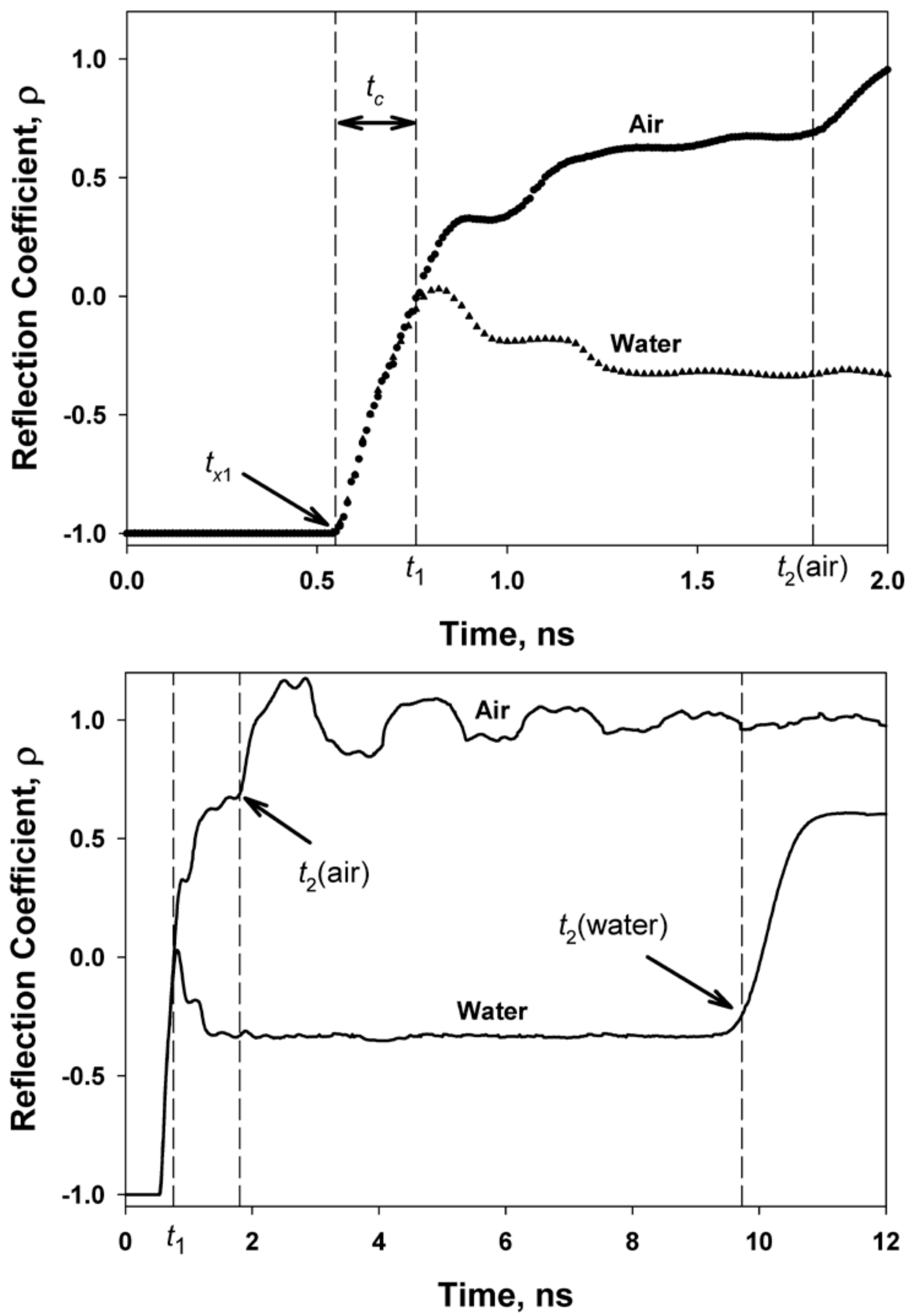

Fig. 2. Waveforms in air and deionized water acquired using a TDR-315 probe showing the time of the step signal launch (t_{x1}), time at which the signal enters the media (t_1) and the time of the reflection at the end of the rod in air, t_2(air), and water t_2(water) determined using AWIGF (Schwartz et al., 2014). The offset, t_c, is fitted based on the calibration in air and water.

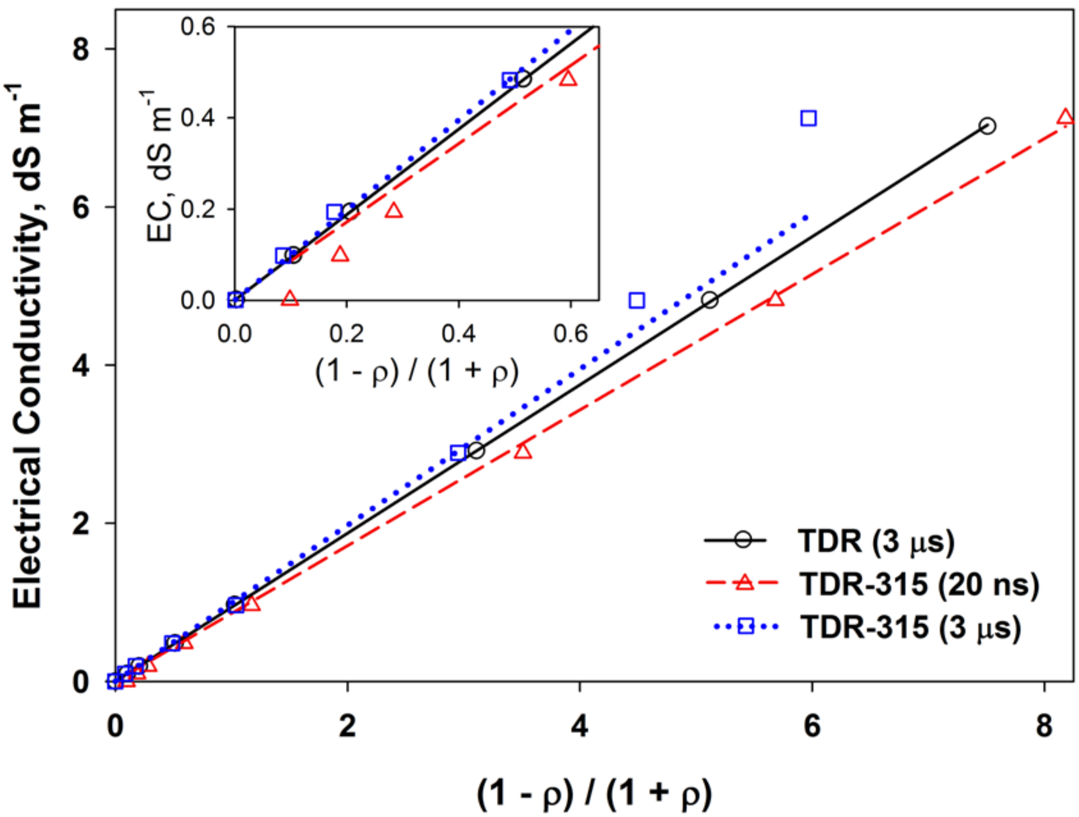

463 Fig. 3. Electrical conductivity (EC) calibrations for the long time reflection coefficient, ρ, in
464 $CaCl_2$ solutions for the TDR and TDR-315. Inset shows calibration response at low EC levels.

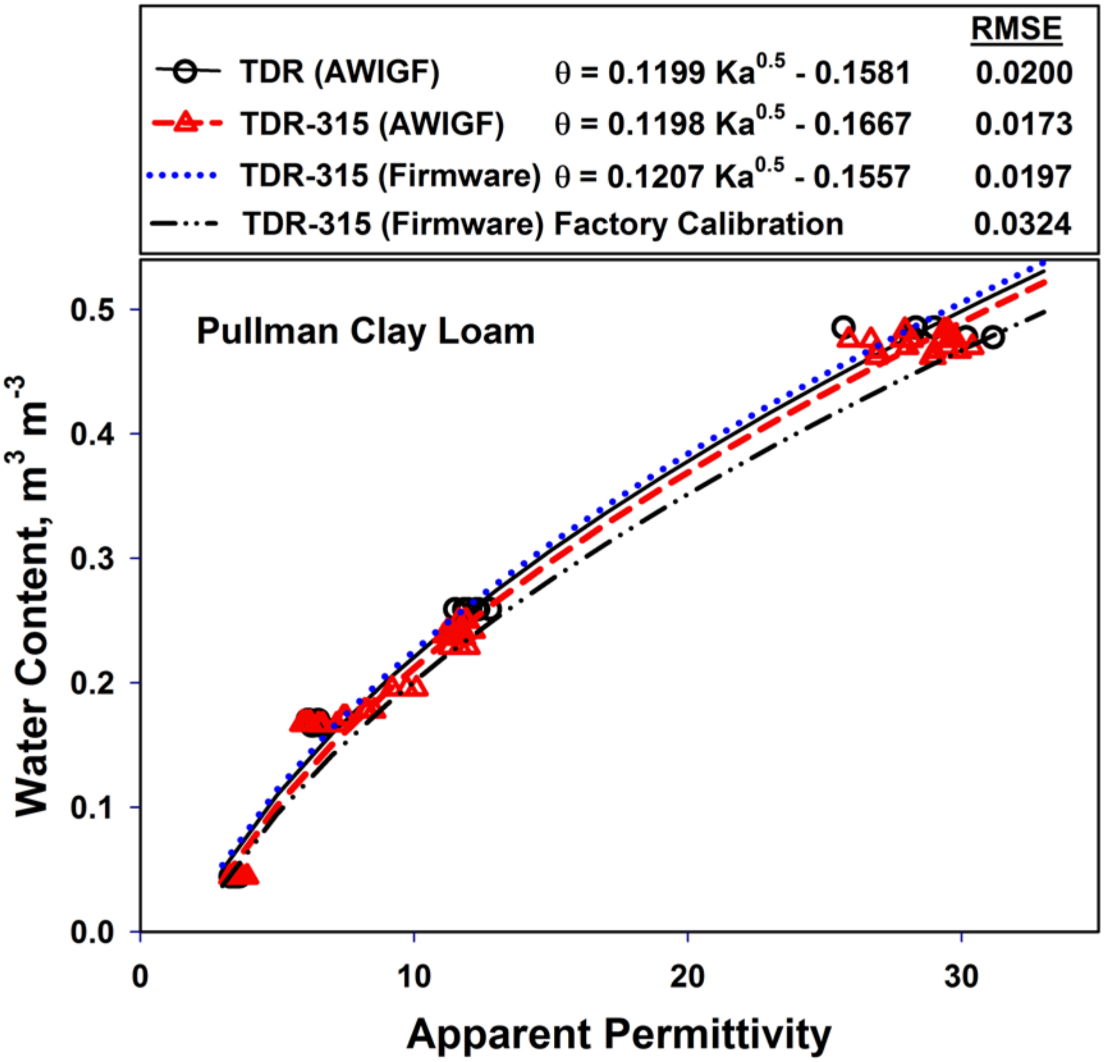

Fig. 4. Refractive mixing model soil water content calibrations of the Pullman clay loam (0.0 to 0.15 m) for conventional TDR and TDR-315 using AWIGF-estimated travel times and the apparent permittivity (K_a) calibration (Fig. 2) and the TDR-315 using firmware estimated K_a. Calibrations include permittivity measurements at all three temperature regimes. Also shown is the Acclima factory soil water content calibration.

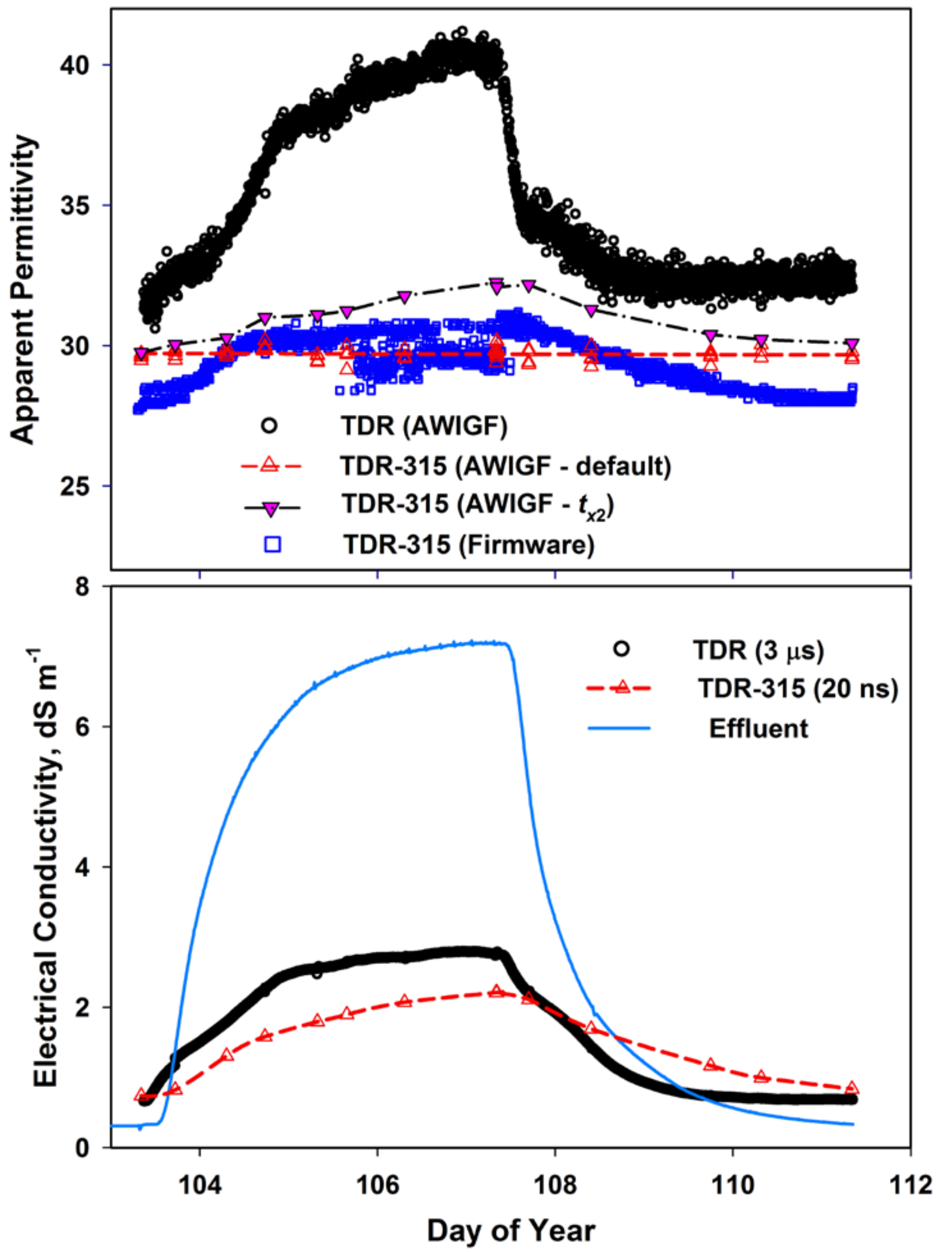

Fig. 5. Response of electrical conductivity and apparent permittivity during column displacement for conventional TDR and TDR-315 sensors in a Pullman clay loam. Apparent permittivities for the TDR-315 are plotted using two AWIGF methodologies to estimate the time at which the pulse arrives at the end of the transmission line (t_2): the default method that uses the maximum of the second derivative and the conventional method that uses the intersection of the tangents to the baseline and rising limb (t_{x2}). In addition, firmware-calculated apparent permittivities are also plotted. A lag in the TDR-315 response compared with conventional TDR is due to differing heights within the soil column.

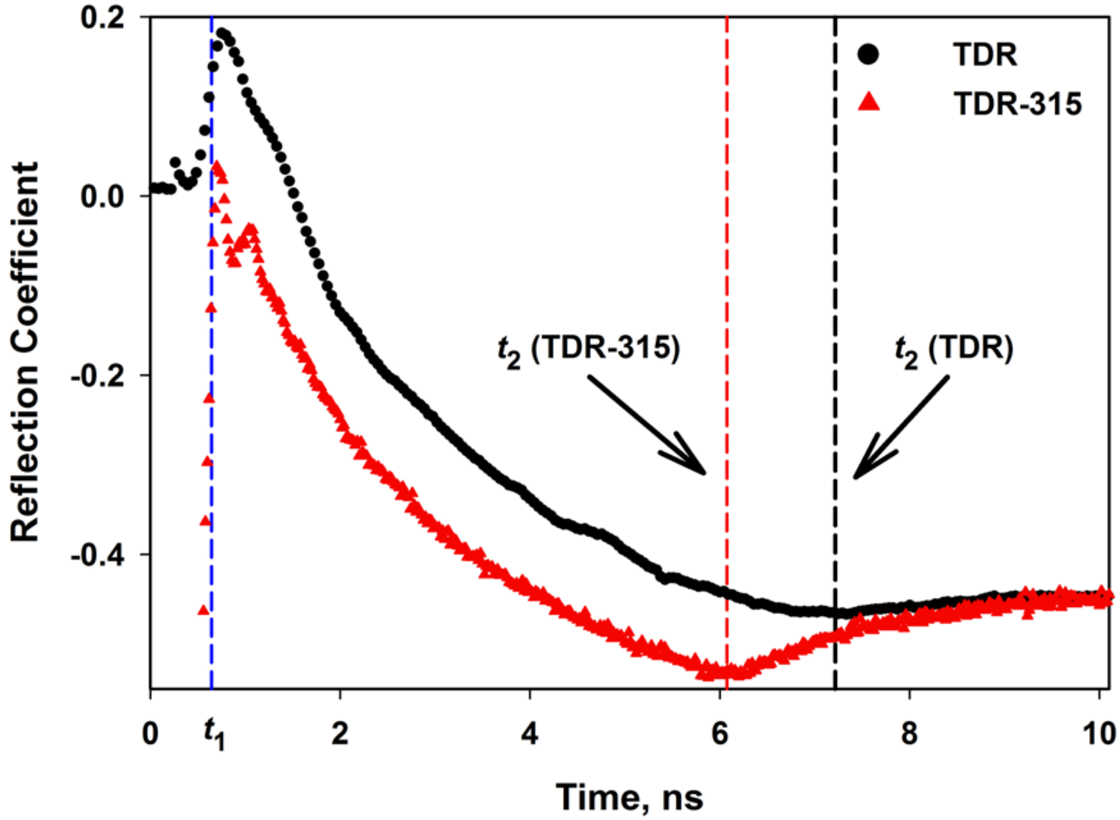

Fig. 6. Waveforms of conventional TDR and the TDR-315 at a bulk electrical conductivity (σ_a) of 2.8 dS m^{-1} and the AWIGF-evaluated time at which the pulse arrives at the end of the transmission line (t_2). The waveforms have been horizontally adjusted in time so that the time at which the step pulse enters the media (t_1) is identical.